ISSN 1541-308X, Physics of Wave Phenomena, 2011, Vol. 19, No. 1, pp. 1–6. © Allerton Press, Inc., 2011.

ULTRASONICS

Simulation of Thermal Lesions in Biological Tissues Irradiated by High-Intensity Focused Ultrasound through the Rib Cage

S. A. Ilyin[1*], S. M. Bobkova[1], V. A. Khokhlova[1***], and L. R. Gavrilov[2]**

[1] *Lomonosov Moscow Sate University, Leninskie Gory 1/2, Moscow, 119991 Russia*

[2] *Andreyev Acoustics Institute, Russian Academy of Sciences, ul. Shvernika 4, Moscow, 117036 Russia*

Received September 2, 2010

Abstract—Thermal effect of high-intensity focused ultrasound on biological tissue behind the rib cage phantom has been numerically simulated. A phased array was used as a source of ultrasound. Temperature and thermal dose distributions in the biological tissue were calculated and used to find the form of thermal lesions. The results of the calculations are in good agreement with experiment and show that the model is applicable for predicting the effect produced by ultrasound in tissue.

DOI: 10.3103/S1541308X11010018

1. INTRODUCTION

Noninvasive (i.e., without surgical intervention) operations are of great interest for cancer therapy. One of the ways to carry out an operation like that is to irradiate a tumor by focused high intensity ultrasound [1, 2]. The region under irradiation is heated by ultrasound to a temperature above 60°C in a few seconds, and thermal necrosis of biological tissue takes place. This allows local lesion of the tumor without damaging the surrounding normal organs and tissues [1, 2]. Now operations of this kind are successfully carried out in clinics in China, the United States, the European Union, and Russia to treat soft tissue tumors in various organs [1].

Wider application of this technique is substantially hindered by the fact that many vital human organs are shielded with bones, which are strongly reflecting and absorbing obstacles. Examples are the liver and rib cage bones, the brain and scull bones. In these cases, when ultrasound is focused on the chosen tissue region, a large part of the energy is absorbed by bones. This results in insufficient heating of the tumor and also in overheating of bones and higher tissue layers, including skin [3].

Modern phased arrays used as radiators have made it possible to solve the problem of decreasing the effect of ultrasound on bones and delivering sufficient ultrasound energy to the focus. Let us consider, as an example, irradiation of the liver located behind the ribs. To solve the problem, we proposed [4] a technique based on switching off the phased array elements shielded by the ribs, which allowed us to shape the focused ultrasound beam in such a way that it passed through the acoustic windows between the ribs, appreciably decreasing the heating of the bones. Experiments confirmed safety of the technique during *in vitro* irradiation and showed a possibility of producing lesions in biological tissue [4]. The purpose of this work was numerical simulation of the thermal effect produced by the high-intensity focused ultrasound on biological tissue located behind the rib cage phantom, comparison of the calculations and experiment [4], and investigation into applicability of the model for predicting results of ultrasound effect on tissue.

In the publications on high-temperature hyperthermia and ultrasound surgery, the result of the thermal effect on tissue is usually evaluated on the basis of the thermal dose concept proposed in [5]. In hyperthermia, the threshold thermal dose necessary for thermal lesion to occur is considered to be the dose allowing the temperature $T = 43°C$ to be maintained in tissue for 120–240 min [5]. With high-intensity focused ultrasound, the irradiation time is much shorter (several seconds), the temperatures attained in the focal region within this time are higher than 60°C, and thermal necrosis of cells occurs almost instantaneously. For these irradiations regimes, it is more convenient to determine the thermal dose with respect to a higher temperature. In this work, the reference point was taken to be $T = 56°C$. When this temperature is maintained for 1 s, the thermal dose equivalent to 140 min at 43°C is obtained [1, 6].

*E-mail: sergey_ilyin@acs366.phys.msu.ru

**E-mail: bobkova-s@mail.ru

***E-mail: vera@acs366.phys.msu.ru

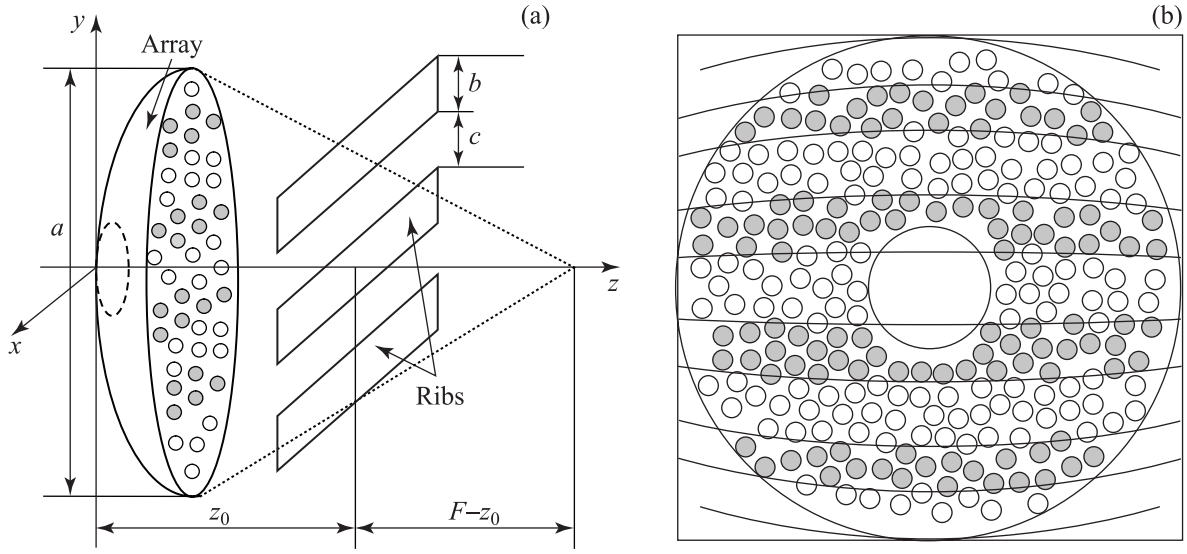

Fig. 1. (a) Geometry of the passage of focused ultrasound through the rib cage and (b) schematic arrangement of active (filled circles) and switched-off (open circles) elements on the array surface.

In the simulation, the biological tissue parameters varied within the range known from the literature in order to get the maximum agreement with experiment [7].

2. EXPERIMENT

Experimental investigations were carried out at the National Physical Laboratory (Teddington, United Kingdom) [4]. The layout of the experiment on the passage of focused ultrasound through the rib cage is shown in Fig. 1(a). The source of ultrasound was a two-dimensional phased array with elements randomly arranged on its surface. The main parameters of the array are as follows: frequency 1 MHz, 254 elements 7 mm in diameter, diameter $D = 170$ mm, curvature radius $F = 130$ mm, diameter of the hole for the diagnosis transducer 40 mm, active array area about 100 cm^2. The maximum acoustic power of the system was 500 W. The design of the array and the results of the calibration experiments on the study of the ultrasound field generated by the array in water are described in more detail in [8].

The phased array was used to minimize the effect of ultrasound on the ribs and maintain high intensities in the focus. The following approach was proposed to solve the problem. Rays were drawn from the array curvature center (focus) to connect the focal point with the center of each array element (Fig. 1(a)). If the ray crossed a rib, the element was switched off. If the ray passed between the ribs, an oscillation velocity value was set for the element. As a result, a striped distribution of active and inactive elements was obtained on the array surface (Fig. 1(b)); the total power of the system was governed by the totality of the operating elements.

Ribs were simulated by a rib cage phantom, which was a set of five strips 3 mm thick and 18 mm wide made from the Aptflex F48 absorbing material (Precision Acoustics, Dorchester, UK). As ultrasound with the frequency of 1 MHz passed through the layer of this material, the total loss was 25 dB and the reflection was −20 dB. The distance between the strips was 14 mm. These dimensions approximately correspond to typical dimensions of ribs and intercostal spaces in samples of the porcine rib cage.

To demonstrate the possibility of tissue lesions behind the ribs, porcine muscle tissue was irradiated *in vitro* through the rib phantom. The tissue sample was degassed in a special chamber for an hour before the beginning of the experiment. A series of tissue irradiations was carried out at a fixed array power and various exposure times. The results are shown in Fig. 2. Panels *1*–*4* correspond to the exposure times 5, 10, 15, and 20 s at the array power 120 W. The phenomenon of focus splitting, typical of irradiation through the periodic rib structure, is evident from the form of lesions: at the irradiation for $\geqslant$10 s two lateral lesions in the subsidiary intensity maxima are observed in addition to the lesion in the main focus at the array curvature center. This phenomenon is associated with interference of waves from spatially separated sources, which are intercostal spaces.

3. THEORETICAL MODEL

Simulation of the thermal effect of ultrasound on tissue can be conventionally divided into three stages. At the first stage, the acoustic field generated by the

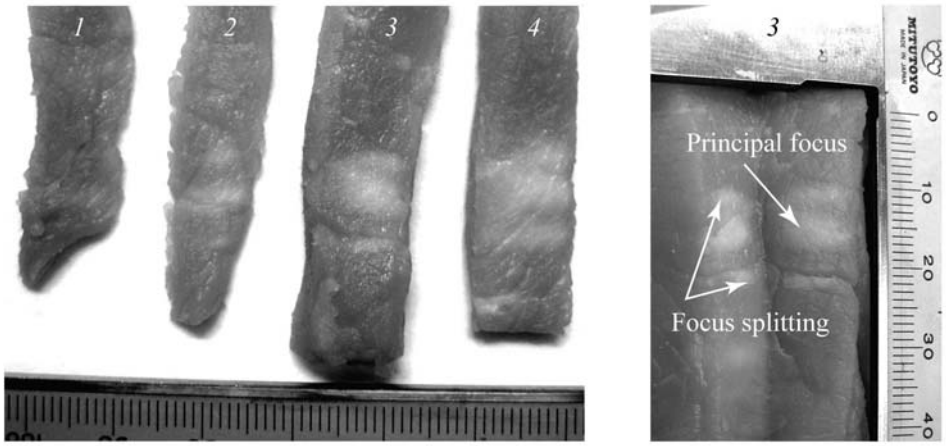

Fig. 2. Photographs of thermal lesions (light areas) in the biological tissue sample in the focal region of the array at the acoustic power 120 W of the array and exposures of 5, 10, 15, and 20 s (*1–4*, respectively).

phased array in water in the focal region is calculated. The results are used at the second stage to calculate intensity and distribution of thermal sources in tissue. At the third stage, the inhomogeneous heat transfer equation was solved and the temperature and thermal dose distributions in the tissue were calculated.

The methods for calculation of acoustic fields generated by phased arrays are described in detail in [9–11]. In the present work, they were modified to apply to the problem of focused ultrasound propagation through the rib cage bones. The calculation of the field was carried on as follows. First, the field of the single array element in water was calculated using the Rayleigh integral:

$$p(x,y,z) = -if\rho \int\limits_S V_0 \frac{\exp(ikR)}{R}\, dS. \qquad (1)$$

Here V_0 is the oscillation velocity amplitude on the surface of the element, $\rho = 1000\,\mathrm{kg\,m^{-3}}$ is the density of the medium, $k = 2\pi f/c$ is the wavenumber, $f = 1\,\mathrm{MHz}$ is the radiation frequency, $c = 1500\,\mathrm{m\,s^{-1}}$ is the speed of sound, R is the radius vector connecting the point at which the field is calculated with the point on the surface of the element, and S is the element surface area over which integration was carried out.

Then the elements shielded by the ribs were switched off and the distribution of the acoustic pressure between the ribs in the $z = z_0$ plane was calculated by summing fields from all active elements of the array (see Fig. 1(a)). Next, with this distribution used as the boundary condition, the pressure distribution in the focal waist was numerically calculated using the Rayleigh integral again:

$$p_{\mathrm{F}}(x,y,z) = \frac{1}{2\pi} \int\limits_S p_{\mathrm{rib}}(x,y,z_0) \times \frac{\exp(ikR)}{R^3}(ikR-1)(F-z_0)\, dx\, dy. \qquad (2)$$

Here R is the radius vector drawn from the point in the plane of the ribs to the focal waist point at which the field was calculated.

Acoustic pressure (2) was used to calculate the intensity I in the approximation of quasi-plane wave propagation:

$$I(x,y,z) = \frac{|p_{\mathrm{F}}(x,y,z)|^2}{2\rho c}. \qquad (3)$$

Numerical calculation of the three-dimensional intensity distribution (1)–(3) took a rather long time. To choose parameters of the numerical mesh and debug the program, preliminary calculations were also performed with the intensity distribution (3) approximated by the Gaussian curves. To choose the approximation constants, the intensity distribution (3) was calculated along three straight lines in the z direction, which run through the centers of the principal and subsidiary maxima, and in the focal region perpendicularly to the direction of the ribs. The approximate intensity distribution in the volume was given by the formula

$$I(x,y,z) = \sum_{j=-1}^{1} I_j \exp\left[-\frac{x^2+(y-jy_0)^2}{r_\perp^2} - \frac{(z-z_{\mathrm{F}})^2}{z_\parallel^2}\right]. \qquad (4)$$

Here $r_\perp = 0.7\,\mathrm{mm}$ and $z_\parallel = 4\,\mathrm{mm}$ are the transverse and longitudinal dimensions of the focal waist, respectively; $y_0 = 4.6\,\mathrm{mm}$ is the y coordinate of the secondary maximum resulting from the periodic rib structure, $z_{\mathrm{F}} = 130\,\mathrm{mm}$ is the position of the focal plane, $I_0 = 1030\,\mathrm{W\,cm^{-2}}$ and $I_{\pm1} = 540\,\mathrm{W\,cm^{-2}}$ are

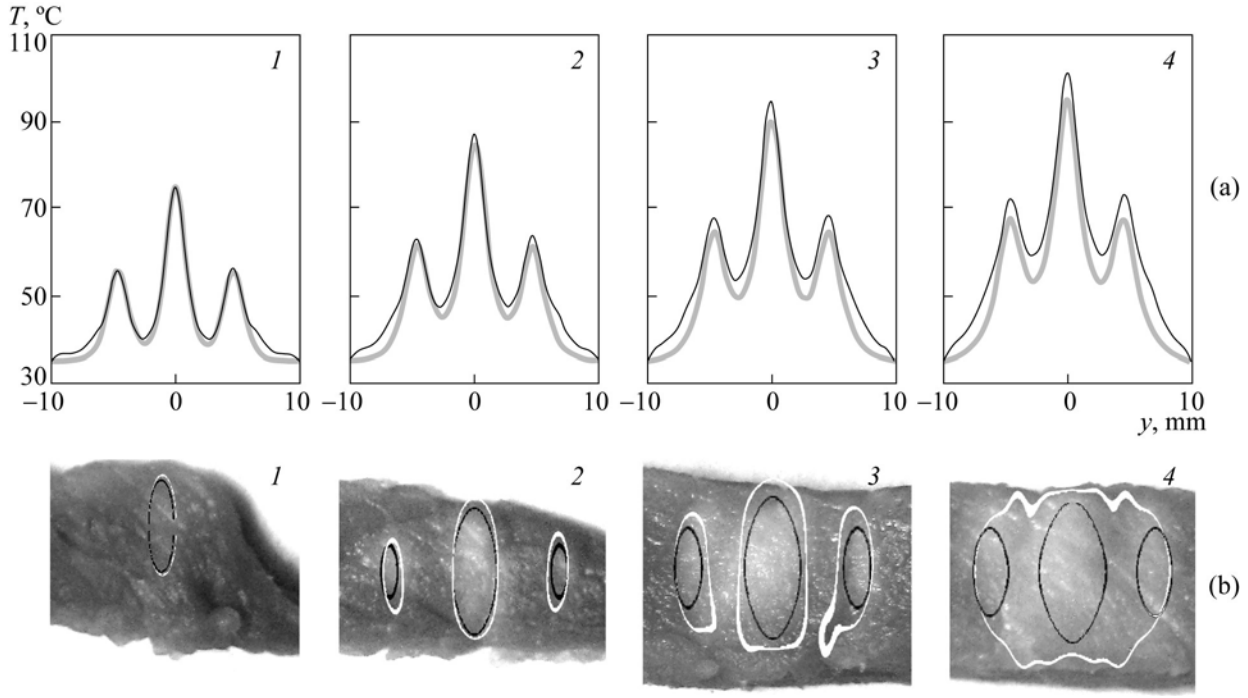

Fig. 3. Results of the numerical simulation of the temperature and thermal dose distributions in the tissue as high-intensity focused ultrasound passes through the ribs. Distributions *1–4* correspond to the acoustic power 120 W of the array and exposures of 5, 10, 15, and 20 s, respectively. (a) Temperature distribution along the y axis in the focal plane for the array field simulated numerically (black lines) and approximated by the Gaussian curves (grey lines). (b) Thermal dose distributions for the array field simulated numerically (white contours) and approximated by the Gaussian curves (black contours).

the intensities in water in the principal and secondary maxima at the total acoustic power 120 W of the array.

The results of the calculations in water were converted to tissue with allowance for attenuation of acoustic energy in the tissue sample:

$$I(x,y,z) = I_{\text{sample}} = I_{\text{water}}(x,y,z)\exp\left[-2\alpha(z-z_1)\right], \quad (5)$$

where z is the coordinate along the focused beam axis (see Fig. 1(a)), $z_1 = 120$ mm is the coordinate of the tissue sample boundary, and α is the sound attenuation coefficient in tissue.

The acoustic intensity field (3) and (4) with allowance for attenuation of ultrasound in tissue (5) was used to calculate the heat deposition rate Q

$$Q(x,y,z) = 2\alpha I \quad (6)$$

and further to simulate the temperature field in the tissue on the basis of the inhomogeneous heat transfer equation

$$\frac{\partial T}{\partial t} = \chi\Delta T + \frac{Q}{c_v}. \quad (7)$$

Here, χ is the thermal diffusivity coefficient, c_v is the heat capacity per tissue unit volume, and $T(t,x,y,z)$ is the temperature in the tissue. The initial temperature value $T_0 = 35°$C corresponded to the experimental conditions. The explicit two-step finite-difference scheme second order accurate in time and spatial coordinates was used in the numerical calculation of temperature (7). The temperature field in the tissue in the course of heating by ultrasound was calculated for the given radiated power of the array and time of irradiation (exposure). The lesion threshold was determined in accordance with the thermal dose value [1, 6]

$$t_{56.0} = \int_0^{t_{\text{heating}}} R_0^{(56.0-T(t))}dt \geqslant 1. \quad (8)$$

Here $t_{56.0}$ is the time equivalent of the thermal dose; the value $t_{56.0} \geqslant 1$ corresponds to tissue lesion; $R_0 = 0.5$ for the temperature above 43°C and $R_0 = 0.25$ for the temperature below 43°C [1, 6]. Thermal lesion was simulated using a number of iterations in which the values for the absorption coefficient, heat capacity, and thermal conductivity varied within the range known from [7] to obtain the maximum agreement of the theoretical and experimental results. The results of the calculations with the parameter values $c_v = 3.06\times10^6$ J m^{-3} °C^{-1}, $\chi = 1.93\times10^{-7}$ m^2 s^{-1}, and $\alpha = 0.42$ dB cm^{-1} MHz^{-1} which allowed good agreement with experiment are listed below.

4. COMPARISON OF THE SIMULATION RESULTS WITH EXPERIMENT

The temperature distributions in tissue obtained with these values of the parameters are shown in Fig. 3(a) for the array field approximated by the Gaussian distributions (grey curves) and the array field calculated by formulas (1)–(3) (black curves). It is seen that at a short heating time (5 s) the temperature distributions almost coincide. At exposures larger than 10 s, there appears difference between the results of the approximate description and direct calculation of the array field. The heat diffusion effect begins to manifest itself at exposures more than 5 s, leading to diffuseness of both the principal and subsidiary maxima, which results in that the lateral focuses begin gradually merging with the main focus.

The thermal necrosis regions of the tissue corresponding to the exposures under consideration are shown in Fig. 3(b). Black lines are the lesion boundaries for the array field approximated by the Gaussian curves, and white lines are the lesion boundaries for the array field directly calculated by formulas (1)–(3). The results of the thermal dose simulation by direct calculation of the array field are in good agreement with the experimental data for all qualitatively different stages of lesion development in time: formation of a single lesion in the main focus (*1*, 5 s), onset of lateral lesion formation (*2*, 10 s), approachment of the main and lateral lesions (*3*, 15 s), and merging of the main and lateral lesions into one (*4*, 20 s). The results of the approximate simulation based on approximation of the array field by the Gaussian distributions of thermal sources are in good agreement with the experimental data at a short exposure (*1*, 5 s), but as heating goes on, the thermal effect is underestimated because the spatial structure of the field and the additional heating between the principal and lateral heat release peaks are ignored.

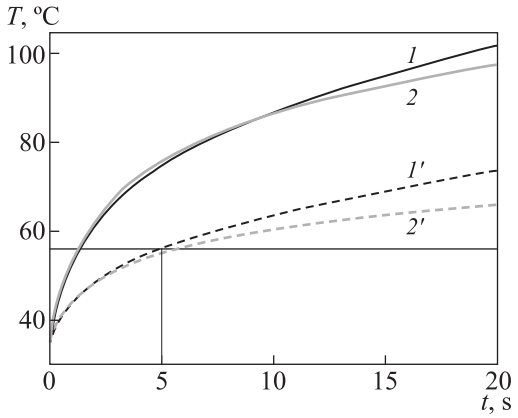

Fig. 4. Temperature increase over time in the principal (curves *1* and *2*) and lateral maxima (curves *1′* and *2′*). Curves *1* and *1′* are for the numerically calculated array field, and curves *2* and *2′* are for the field approximated by the Gaussian curves.

Figure 4 shows variation in temperature with time in the principal and subsidiary maxima of the tissue heating in the focal plane for the numerically calculated array field and for the array field approximated by the Gaussian curves. In the plots, the horizontal line indicates the temperature of 56°C relative to which the tissue lesion threshold was determined. It is evident from the plot that at the exposure of 5 s the temperature of 56°C is attained in the lateral maximum only at the very end of the irradiation and no tissue lesion occurs (line *1′* is direct calculation and line *2′* is approximate calculation). At the exposure of 5 s the temperature is higher than 56°C for more than a second in the principal maximum, and at the exposure of 10 s and longer this is true for all three maxima, i.e., it predicts the onset of lesion formation, which was exactly observed in the experiment.

5. CONCLUSIONS

The results of the numerical simulation presented in this work are in good agreement with the experimental data and demonstrate suitability of the proposed models for preplanning operations in clinical practice and predicting the form of thermal lesions in tissues under the effect of ultrasound.

Direct calculation of the three-dimensional distribution of the field intensity in the tissue in the presence of ribs takes quite a lot of time, but preliminary calculations can be performed using the Gaussian approximation, which describes the temperature field structure at short exposures well.

Using the simulation results, one can determine thresholds for formation of lateral lesions, in addition to those in the central focus, which arise from propagation of ultrasound through ribs. Sometimes, for example, when the size of the irradiated volume is small as compared with the distance between the secondary focuses, this focus splitting can be a limiting factor for the use of this surgical approach. On the contrary, when large-volume tumors are irradiated, secondary lesions and their merging with the central one due to diffusion can allow the single-impact volume to be extended and thus probably play even a positive role.

ACKNOWLEDGMENTS

The authors are grateful to their colleagues J. Hand (Imperial College, London) and A. Shaw (National Physical Laboratory, Teddington, United Kingdom) for the possibility of conducting joint experiments with the random array, and to O.A. Sapozhnikov for helpful discussions of the work.

The work was supported by the UMNIK and the RFBR Projects 09-02-00066, 09-02-01530, and 10-02-91062-PICS.

REFERENCES

1. C. Hill, J. Bamber, and G. ter Haar, *Physical Principles of Medical Ultrasonics*, 2nd ed. (Wiley, Chichester, 2004).
2. M. R. Bailey, V. A. Khokhlova, O. A. Sapozhnikov, S. G. Kargl, and L. A. Crum, "Physical Mechanisms of the Therapeutic Effect of Ultrasound (A Review)," Acoust. Phys. **49**(4), 369 (2003).
3. F. Li, X. Gong, K. Hu, C. Li, and Z. Wang, "Effect of Ribs in HIFU Beam Path on Formation of Coagulative Necrosis in Goat Liver," in *Proceedings of the Therapeutic Ultrasound: 5th International Symposium on Therapeutic Ultrasound (Boston, Massachusetts, 27–29 October 2005)*. AIP Conf. Proc. **829**, 477 (2006).
4. S. Bobkova, L. Gavrilov, V. Khokhlova, A. Shaw, and J. Hand, "Focusing of High Intensity Ultrasound through the Rib Cage Using Therapeutic Random Phased Array," Ultrasound in Medicine and Biology. **36**(6), 888 (2010).
5. S. A. Sapareto and W. C. Dewey, "Thermal Dose Determination in Cancer Therapy," Rad. Oncol. Biol. Phys. **10**, 787 (1984).
6. E. A. Filonenko, L. R. Gavrilov, V. A. Khokhlova, and J. W. Hand, "Heating of Biological Tissues by Two-Dimensional Phased Arrays with Random and Regular Element Distributions," Acoust. Phys. **50**(2), 222 (2004).
7. F. A. Duck, *Physical Properties of Tissue* (Academic Press, London, 1990), p. 346.
8. J. W. Hand, A. Shaw, N. Sadhoo, S. Rajagopal, R. J. Dickinson, and L. R. Gavrilov, "A Random Phased Array Device for Delivery of High Intensity Focused Ultrasound," Phys. Med. Biol. **54**, 5675 (2009).
9. L. R. Gavrilov and J. W. Hand, "A Theoretical Assessment of the Relative Performance of Spherical Phased Arrays for Ultrasound Surgery and Therapy," IEEE Trans. Ultrason. Ferroelec. Freq. Contr. **41**(1), 125 (2000).
10. E. S. Ebbini and C. A. Cain, "Multiple-Focus Ultrasound Phased Array Pattern Synthesis: Optimal Driving Signal Distributions for Hyperthermia," IEEE Trans. Ultrason. Ferroelec. Freq. Contr. **36**(5), 540 (1989).
11. S. A. Goss, L. A. Frizzell, J. T. Kouzmanoff, J. M. Barich, and J. M. Yang, "Sparse Random Ultrasound Phased Array for Focal Surgery," IEEE Trans. Ultrason. Ferroelec. Freq. Contr. **43**(6), 1111 (1996).